

Hybrid Near-Field and Far-Field Localization with Multiple Holographic MIMO Surfaces

Mengyuan Cao, *Student Member, IEEE*.

Abstract—Localization methods based on holographic multiple input multiple output (HMIMO) have gained much attention for its potential to achieve high accuracy. By deploying multiple HMIMOs, we can improve the link quality and system coverage. As the scale of HMIMO increases to improve beam control capability, the near-field (NF) region of each HMIMO expands. However, existing multiple HMIMO-enabled methods mainly focus on the far-field (FF) of each HMIMO, which leads to low localization accuracy when applied in the NF. In this paper, a hybrid NF and FF localization method aided by multiple RISs, a low cost implementation of HMIMO, is proposed. In such a scenario, it is difficult to achieve user localization and RIS optimization since the equivalent NF of all RISs expands, which results in high complexity, and we need to handle the interference caused by multiple RISs. To tackle this challenge, we propose a two-phase RIS-enabled localization method that first estimate the relative locations of the user to each RIS and fuse the results to obtain the global estimation. In this way, the algorithm complexity is reduced. We formulate the RIS optimization problem to keep the RIS sidelobe as low as possible to minimize the interference. The effectiveness of the proposed method is verified through simulations.

Index Terms—Holographic multiple-input multiple-output (HMIMO), reconfigurable intelligent surface (RIS), near-field localization, far-field localization.

I. INTRODUCTION

The growing number of location-dependent services, like navigation systems, user monitoring, and autonomous vehicles, has increased the need for precise localization. This surge in demand has inspired the exploration of innovative localization methods. Among them, holographic multiple input multiple output (HMIMO)-based localization has gained significant attention due to its potential to achieve high localization accuracy. Specifically, HMIMO is capable of manipulating electromagnetic (EM) fields and generate desirable beams with high precision due to its massive number of tunable elements [1] [2].

When facing a large localization area, it is hard for a single HMIMO to efficiently deal with all possible user locations. By deploying multiple HMIMOs over the area of interest, the link quality and coverage can be greatly enhanced [3]. In the literature, some existing works have considered the localization systems aided by multiple HMIMOs. In [4], a two-stage user localization method based on the atomic norm minimization and least-squares line intersection is proposed to leverage the multi-reflection wireless environment. The authors in [5] proposed a method that jointly estimates the time of arrival and angle of arrival of signals through HMIMOs and then uses the time difference of arrival to locate the user.

However, these methods mainly focus on the localization in the far-field (FF) of each HMIMO. Due to the large size of the HMIMO, the near-field (NF) region of each HMIMO is expanded. In NF, the traditional plane wave model applied in the FF fails to characterize the signal propagation accurately, and we need to apply the spherical wave model. In practical scenarios, users may exist in both the NF and FF regions of the HMIMO. Hence, a hybrid localization scheme is required to adapt to both the NF and FF regions.

In this paper, a localization scheme based on multiple HMIMOs is proposed where a single base station (BS) and multiple reconfigurable intelligent surfaces (RISs) are coordinated to serve multiple users in hybrid near- and far-field. An RIS is composed of multiple sub-wavelength nearly-passive scattering elements [6], and is a low-cost implementation of HMIMO. Specifically, in the localization process, the RISs reflect the signals emitted from several single-antenna users to the BS. The BS then utilizes the signals reflected by the selected RIS for each user to obtain the localization results. Subsequently, the RIS selection and their phase shifts are optimized based on the estimated locations of the users. The location estimation and RIS optimization are performed iteratively to improve localization accuracy.

Several challenges need to be addressed for the proposed localization scheme. *First*, for multiple RISs, the equivalent NF, which refers to the equivalent NF applicable to all RISs collectively, is expanded. Therefore, using all received signals simultaneously to locate the user results in high complexity, which leads to difficulty in designing the localization algorithm. *Second*, the received signal could contain the signal reflected multiple times by different RISs, which causes interference between RISs.

Therefore, the main contributions of this paper can be summarized in the following:

- We consider a multiple RIS-aided hybrid NF and FF localization scenario to enhance the system coverage and link quality. A hybrid NF and FF localization protocol is proposed to coordinate the operations of the BS, the RISs, and the users.
- We design a two-phase localization algorithm to reduce complexity. The locations for each selected RIS is estimated and then fused to obtain the global localization results. The RIS selection for each user and their phase shifts are optimized. An algorithm based on the alternating direction method of multipliers is designed to obtain optimal RIS phase shifts.
- The performance of the proposed method and other RIS-based localization algorithms are compared. Simulation

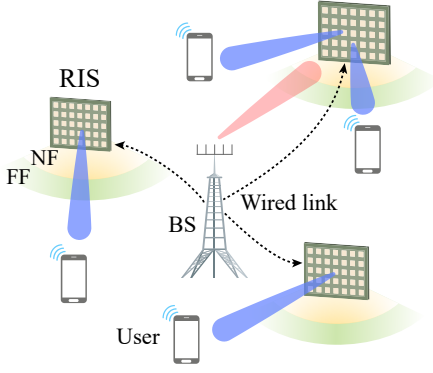


Fig. 1. Hybrid NF and FF localization aided by multiple BSs and RISs.

results show that the proposed approach outperforms other methods by more than 40% in the RMSE when $\text{SNR} > 5$. We also reveal the complexity and localization accuracy advantage of the hybrid model compared with the pure NF or FF model.

The rest of the paper is organized as follows. In Sec. II, we introduce the localization scenario, the channel model, and the localization protocol. The localization algorithm is proposed in Sec. III. Then, the RIS optimization algorithm is designed in Sec. IV. In Sec. V, we present the simulation results. Finally, conclusions are drawn in Sec. VI.

II. SYSTEM MODEL

In this section, we first describe the localization scenario, and then introduce the signal model and the localization protocol for the proposed scenario.

A. Localization Scenario

As shown in Fig. 1, we consider a wireless localization network consisting of a BSs, K single-antenna users and M RISs. The BS is equipped with Q antennas. Each RIS contains $N = N_1 \times N_2$ reflecting elements with tunable phase shifts.

During the localization, the RISs that offer more reliable connections to each user are selected to locate each user. The BS separates the signal reflected by each RIS by digital beamforming, and performs localization for each user using the signals reflected by its selected RIS. The RIS selection and phase shifts are iteratively optimized based on the fused localization results to improve the localization accuracy. To avoid multi-user interference, frequency division multiplexing (FDM) is applied to transmit signals from different users. Note that each user can be in either the NF or the FF region of each RIS, and which region a user locates in is unknown.

B. Channel Model

The channel between the k -th user and the BS via the m -th RIS can be given by [7]

$$\mathbf{h}_{km}(\mathbf{p}_k^m) = (\mathbf{H}_m^A)^T \text{diag}\{\boldsymbol{\beta}_m\} \mathbf{h}_{km}^t(\mathbf{p}_k^m), \quad (1)$$

where $\boldsymbol{\beta}_m = [\beta_1^m, \dots, \beta_N^m]^T \in \mathbb{C}^{N \times 1}$ is the phase shift vector of the m -th RIS with β_n^m being the phase shift of the n -th RIS element of the m -th RIS. $\mathbf{p}_k^m = [r_k^m, \theta_k^m, \phi_k^m]^T$ is the

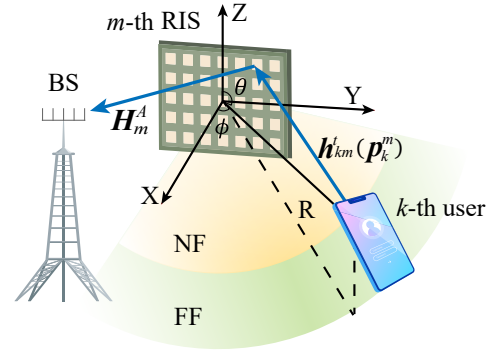


Fig. 2. Illustration of the channel between a user and a BS.

relative location of the k -th user to the m -th RIS. $\mathbf{H}_m^A \in \mathbb{C}^{N \times Q}$ represents the channel between the m -th RIS and the BS, and $\mathbf{h}_{km}^t(\mathbf{p}_k^m)$ is the channel between the m -th RIS and the k -th user, as illustrated in Fig. 2. In the following, we give the expressions of RIS-user channels of the NF and FF users, respectively.

Channel Models for the NF Region: When the user is located in the NF region of the m -th RIS, we adopt the spherical wave model to describe the signal received by the RIS. Thus, the channel between the k -th user and the m -th RIS is given by [8]

$$\mathbf{h}_{km}^t(\mathbf{p}_k^m) = \alpha_{km} \mathbf{b}(r_k^m, \theta_k^m, \phi_k^m), \quad \mathbf{p}_k^m \in \mathbf{D}_{NF}^m, \quad (2)$$

where α_{km} is the channel gain [9]. \mathbf{b} is the steering vector in the NF region and can be given as

$$\mathbf{b}(r_k^m, \theta_k^m, \phi_k^m) = \left[\exp\left(-j \frac{2\pi}{\lambda} d_{km1}^t\right), \dots, \exp\left(-j \frac{2\pi}{\lambda} d_{kmN}^t\right) \right]^T, \quad (3)$$

where d_{kmn}^t is the distance between the k -th user and the n -th RIS element of the m -th RIS. \mathbf{D}_{NF}^m represents the NF region of the m -th RIS [10].

Channel Models for the FF Region: When the user is located in the FF region, the wavefront can be approximated as a plane. Thus, the received signals are described using the plane wave model, and the user-RIS channel can be given by [11]

$$\mathbf{h}_{km}^t(\mathbf{p}_k^m) = \alpha_{km} \mathbf{a}(\theta_k^m, \phi_k^m), \quad \mathbf{p}_k^m \in \mathbf{D}_{FF}^m, \quad (4)$$

where $\mathbf{a}(\theta, \phi)$ is the steering vector in the FF region and can be given as

$$\mathbf{a}(\theta, \phi) = \left[\exp\left(-j \frac{2\pi}{\lambda} (-y_1 \sin \theta \sin \phi - z_1 \cos \theta)\right), \dots, \exp\left(-j \frac{2\pi}{\lambda} (-y_N \sin \theta \sin \phi - z_N \cos \theta)\right) \right]^T, \quad (5)$$

where $(0, y_n, z_n)$ is the coordinate of the n -th RIS element in its local coordinate. \mathbf{D}_{FF}^m represents the FF region of the m -th RIS [10].

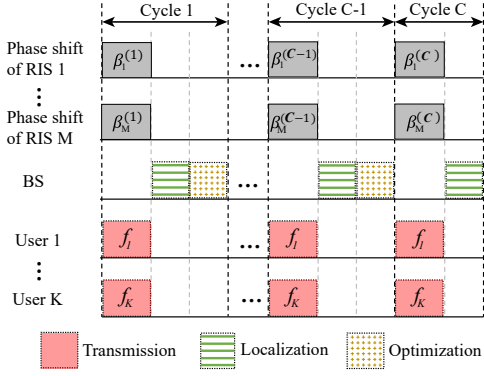


Fig. 3. RIS-enabled hybrid NF and FF source localization protocol.

C. Localization Protocol

A localization protocol is designed for the localization system aided by multiple RISs. The localization process is composed of C cycles, and each cycle contains three steps: transmission, localization, and optimization. The process of the localization protocol is illustrated in Fig. 3, and the steps in each cycle are elaborated in the following.

1) *Transmission*: In this step, the users broadcast signals to the surroundings, and the BS receives signals reflected by the RISs. Let $\mathbf{G}_m^{(c)} = [\mathbf{g}_{m1}^{(c)}, \dots, \mathbf{g}_{mK}^{(c)}]^T$ denote the signal reflected by the m -th RIS and received by the BS in the c -th cycle.

2) *Localization*: In the next step, the BS first estimates each user's location using the received signals reflected by each user's selected RISs, denoted by $\hat{\mathbf{P}}^{(c)} = [\hat{\mathbf{p}}_1^{(c)}, \dots, \hat{\mathbf{p}}_K^{(c)}]$. The details of the localization algorithm are introduced in Sec. III.

3) *Optimization*: In the last step of the c -th cycle, the BS first optimize the RIS selection for each user, and then determines the optimal RIS phase shifts $\beta_m^{(c+1)}$ according to $\hat{\mathbf{P}}^{(c)}$ and the RIS selection results. Note that this step is not executed in the last cycle. The details of optimization algorithm are introduced in Sec. IV.

III. MULTIPLE RIS-ENABLED LOCALIZATION

In this section, a two-phase localization strategy is proposed for the localization step in each cycle of the protocol. Specifically, in Subsection III-A, we introduce the localization method for using the signals reflected by the selected RISs to estimate the user locations independently. Next, in Subsection III-B, the method to fuse all the local localization results is designed.

A. Independent Localization

In this subsection, we first formulate the independent localization problem, and then an independent localization algorithm is proposed to solve the formulated problem efficiently.

1) *Localization Problem Formulation*: We formulate the multi-user localization problem to minimize the localization loss, which is defined as the sum of the l_2 -norm of the residual between the received signals and the signals reconstructed by

using the estimated locations. Thus, the localization problem can be given by

$$\text{P1} : \min_{\tilde{\mathbf{p}}_k^m} \sum_{i=1}^c \left\| \mathbf{g}_{mk}^{(i)} - (\mathbf{H}_m^A)^T \text{diag}\{\beta_m^{(i)}\} \mathbf{h}_{km}^t (\tilde{\mathbf{p}}_k^m) s_k \right\|_2^2, \quad (6a)$$

$$\text{s.t. } \tilde{\mathbf{p}}_k^m \in \mathcal{D}, k \in \mathcal{K}_m^i, \quad (6b)$$

where s_k is the narrowband signal transmitted by the k -th user, \mathcal{K}_m^i represents the set of users that selected m -th RIS in the i -th cycle. $\mathbf{g}_{mk}^{(c)} \in \mathbb{C}^{c \times 1}$ is the signal transmitted by the k -th user, reflected by m -th RIS and received by the BS in the previous c cycles. \mathcal{D} is the whole search area.

2) *Localization Algorithm*: To solve (P1), we propose a location estimation algorithm based on orthogonal matching pursuit (OMP), a classic sparse recovery algorithm. Specifically, we first sample the search domain in NF and FF regions in the local coordinate of each RIS. Considering the different signal models in the NF and FF, we sample the angle and range for NF, and only the angle for FF. Here, range, azimuth and elevation angles are sampled uniformly, with sampling spacing $\Delta R, \Delta \theta, \Delta \phi$, respectively. The sampled locations are given by $\mathbf{Z} = [\mathbf{Z}_{near}, \mathbf{Z}_{far}]$, where

$$\mathbf{Z}_{near} = [(r_1^m, \theta_1^m, \phi_1^m)^T, \dots, (r_{S_1}^m, \theta_{S_1}^m, \phi_{S_1}^m)^T], \quad (7)$$

$$\mathbf{Z}_{far} = [(\theta_1^m, \phi_1^m)^T, \dots, (\theta_{S_2}^m, \phi_{S_2}^m)^T], \quad (8)$$

where S_1 and S_2 are the total number of sampled NF and FF locations. Then, the steering vectors of the sampled locations form the atom channels $\mathbf{F} = [\mathbf{F}_{near}, \mathbf{F}_{far}]$, which is given by [10]

$$\mathbf{F}_{near} = [\mathbf{b}(r_1^m, \theta_1^m, \phi_1^m), \dots, \mathbf{b}(r_{S_1}^m, \theta_{S_1}^m, \phi_{S_1}^m)], \quad (9)$$

$$\mathbf{F}_{far} = [\mathbf{a}(\theta_1^m, \phi_1^m), \dots, \mathbf{a}(\theta_{S_2}^m, \phi_{S_2}^m)], \quad (10)$$

where $\mathbf{b}(r_s^m, \theta_s^m, \phi_s^m)$ is the NF steering vector if the user is located in $(r_s^m, \theta_s^m, \phi_s^m)$, and $\mathbf{a}(\theta_s^m, \phi_s^m)$ is the FF steering vector given the FF location (θ_s^m, ϕ_s^m) .

Hence, (P1) can be approximated as

$$\text{P1}' : \min_{\mathbf{u}_k} \sum_{i=1}^c \left\| \mathbf{g}_{mk}^{(i)} - (\mathbf{H}_m^A)^T \text{diag}\{\beta_m^{(i)}\} \mathbf{F} \mathbf{u}_k s_k \right\|_2^2, \quad (11a)$$

$$\text{s.t. } \|\mathbf{u}_k\|_0 = 1, k \in \mathcal{K}_m^i, \quad (11b)$$

where \mathbf{u}_k is the amplitude of the atom channels \mathbf{F} for the k -th user, which is a 1-sparse vector since we only consider the direct user-RIS path. Hence, (P1') can be solved by OMP. Specifically, suppose $\tilde{\mathbf{u}}_k$ is the solution of (P1'), and the index of its non-zero element is i , the estimated location of the k -th user can be given by

$$\tilde{\mathbf{p}}_{mk} = \begin{cases} [r_i^m, \theta_i^m, \phi_i^m]^T, & (i \leq S_1), \\ [\theta_{i-S_1}^m, \phi_{i-S_1}^m]^T, & (i > S_1). \end{cases} \quad (12)$$

B. Location Fusion

After the BS independently estimate the local locations of all the users, the estimation results are fused to obtain a more accurate global estimation of user locations. We define a fusion loss as the sum of squared relative distances between the global

estimated location and all the local estimated locations. Since the local estimation results in NF and FF regions have different forms, i.e., with or without range information, we need to separately calculate the relative distances for NF and FF cases.

NF case: Suppose the BS estimates that the k -th user is located in the NF of the m -th RIS, then the relative distance can be given as:

$$d_{mk} = \|\hat{\mathbf{p}}_k - \tilde{\mathbf{p}}_k^m\|. \quad (13)$$

where $\hat{\mathbf{p}}_k$ is the global estimated location of the k -th user, and $\tilde{\mathbf{p}}_k^m = [\tilde{r}_{mk}, \tilde{\theta}_{mk}, \tilde{\phi}_{mk}]^T$ is its local location estimated by the m -th BS.

FF case: The FF localization result only contain angle information and corresponds to a ray in 3D space. Thus, we define the relative distance in this case as the minimum distance from the estimated global location to the ray, which is given as

$$d_{mk} = \|\overrightarrow{A_m P_k} \times \overrightarrow{A_m B_{mk}}\|, \quad (14)$$

where $\overrightarrow{A_m P_k}$ is the vector from the m -th RIS to the estimated global location of the k -th user. $\overrightarrow{A_m B_{mk}}$ is the unit vector parallel to the estimated FF direction $\tilde{\mathbf{p}}_k^m = [\theta_k^m, \phi_k^m]$.

Therefore, the fusion problem for the k -th user can be formulated as

$$\text{P2: } \min_{\hat{\mathbf{p}}_k} f(\hat{\mathbf{p}}_k) = \sum_{m \in \mathcal{M}_k} d_{mk}^2(\hat{\mathbf{p}}_k) \quad (15a)$$

$$\text{s.t. } \hat{\mathbf{p}}_k \in \mathcal{D}, \quad (15b)$$

where \mathcal{M}_k represents the set of the selected RISs for the k -th user. For simplicity, we consider a rectangular space. Then, its closed-form solution can be derived by quadratic programming.

IV. RIS OPTIMIZATION

In this section, we first formulate the RIS phase shift optimization problem for the optimization step in each cycle of the protocol. Then, an optimization algorithm based on alternating direction method of multipliers (ADMM) is proposed to solve the formulated problem.

A. RIS Selection Optimization

After obtaining the global estimated locations for all user, we select L RISs with the highest channel gain to serve each user [12]. Since the channel gain between the RIS and the user is negatively related to their relative distance \hat{r}_{km} , we choose L RISs with the minimum distances.

Then the problem can be formulated as

$$\text{P3: } \min_{\mathcal{M}_k} \sum_{m \in \mathcal{M}_k} \hat{r}_{km}, \quad (16a)$$

$$\text{s.t. } |\mathcal{M}_k| = L, \quad (16b)$$

where $|\cdot|$ represents the number of elements in a set. The above problem can be solved directly by calculating the distance $\hat{r}_{km} = \|\mathbf{q}_m - \hat{\mathbf{p}}_k\|$, where \mathbf{q}_m is the location of the m -th RIS.

B. Phase Shift Optimization

1) *Problem Formulation:* In the optimization step, the BS optimizes the RIS phase shifts based on the global localization results. The primary optimization metric is the Cramér-Rao Bound (CRB), which is a standard for evaluating the error in parameter estimation. Additionally, to minimize the interference between RISs, we aim to limit the RIS sidelobe amplitude directed towards other RISs. This approach also aligns with the localization problem formulation, where the user-RIS paths through multiple RIS reflections are ignored. Hence, the objective is to minimize the weighted sum of CRBs of the range and angle estimation errors for all users while keeping the RIS sidelobe as low as possible, and thus the optimization problem can be formulated as

$$\text{P4: } \min_{\beta_m^{(c+1)}, \eta} \epsilon \log \eta + \sum_{k \in \mathcal{K}_m} \text{tr}(\mathbf{J}_{mk}^{-1}) \quad (17a)$$

$$\text{s.t. } |\beta_{mn}^{(c+1)}| = 1, \forall n, \quad (17b)$$

$$|(\mathbf{h}_{mq}^A)^T \text{diag}\{\beta_m^{(c+1)}\} \mathbf{a}(\theta_{im}, \phi_{im})|_2^2 \leq \eta, i \neq m, \forall q \quad (17c)$$

where $\beta_m^{(c+1)} = [\beta_{m1}^{(c+1)}, \dots, \beta_{mN}^{(c+1)}]^T$ is the phase shift of the m -th RIS in the $(c+1)$ -th cycle, with each element satisfying the constant modulus constraint (17b). Here, \mathbf{J}_{mk} is the Fisher information matrix of \mathbf{p}_k , which is a function of the RIS phase shifts $\beta_m^{(c+1)}$ and can be calculated according to [10]. ϵ is the penalty factor to balance the impact of maximum allowed sidelobe amplitude η . (17c) is the sidelobe suppression constraint. It ensures that the radiation pattern $(\mathbf{h}_{mq}^A)^T \text{diag}\{\beta_m\} \mathbf{a}(\theta_{im}, \phi_{im})$ of the angle (θ_{im}, ϕ_{im}) is below η [13], where \mathbf{h}_{mq}^A is the channel between the q -th antenna of the BS and the m -th RIS. Here, we assume each RIS lies in the FF region of other RISs, and $\{(\theta_{im}, \phi_{im})\}_{i \neq m}$ are the relative angles of other RISs for the m -th RIS. In this way, the user-RIS path formed by multiple RIS reflections can be neglected.

2) *Algorithm Design:* An ADMM-based algorithm is designed to solve the formulated problem. We introduce the auxiliary variables $\mathbf{g} = \{g_{iq}\}_{i \neq m, \forall q}$, which is defined as $g_{iq} = (\mathbf{h}_{mq}^A)^T \text{diag}\{\beta_m^{(c+1)}\} \mathbf{a}(\theta_{im}, \phi_{im})$. Therefore, the partial augmented Lagrangian of the formulated problem can be given by [13]

$$L_\gamma = \epsilon \log \eta + \sum_{k \in \mathcal{K}_m} \text{tr}(\mathbf{J}_k^{-1}) + \frac{\gamma}{2} \sum_{i \neq m, \forall q} (|g_{iq} - (\mathbf{h}_{mq}^A)^T \text{diag}\{\beta_m^{(c+1)}\} \mathbf{a}(\theta_{im}, \phi_{im}) + \lambda_{iq}|^2 - |\lambda_{iq}|^2), \quad (18)$$

where γ is penalty factors, λ_{iq} is scaled dual variable with $i \neq m, \forall q$. Then, we iteratively solve the variables $\beta_m^{(c+1)}$, \mathbf{g} , η and $\{\lambda_{iq}\}$. For simplicity, $\beta_m^{(c+1)}$ is denoted as β in the

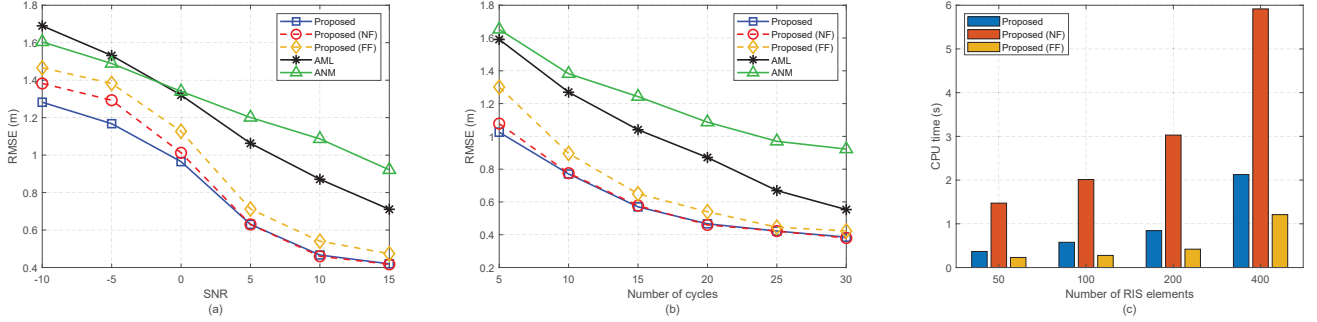


Fig. 4. (a) Average estimation accuracy of the proposed algorithm for different SNR compared with AML and ANM. (b) Average estimation accuracy of the proposed algorithm for different number of localization cycles compared with AML and ANM. (c) CPU time of the proposed algorithm in hybrid, NF and FF model.

following. The subproblems are given by

$$\begin{aligned} \beta^{t+1} &= \arg \min_{\beta} L_{\gamma}(\beta, \mathbf{g}^t, \eta^t, \lambda_{iq}^t), \\ s.t. |\beta_n| &= 1, \end{aligned} \quad (19a)$$

$$\begin{aligned} \{\mathbf{g}^{t+1}, \eta^{t+1}\} &= \arg \min_{\mathbf{g}, \eta} L_{\gamma}(\beta^{t+1}, \mathbf{g}, \eta, \lambda_{iq}^t), \\ s.t. |g_{iq}|^2 &\leq \eta, \end{aligned} \quad (19b)$$

$$\lambda_{iq}^{t+1} = \lambda_{iq}^t + g_{iq}^{t+1} - (\mathbf{h}_{mq}^A)^T \text{diag}\{\beta^{t+1}\} \mathbf{a}(\theta_{im}, \phi_{im}). \quad (19c)$$

Solution to (19a): Define $v_{iq} = g_{iq} + \lambda_{iq}$ and $\mathbf{w}_{iq}^T = (\mathbf{h}_{mq}^A)^T \text{diag}\{\mathbf{a}(\theta_{im}, \phi_{im})\}$, we can rewrite (19a) as

$$\min_{\beta} \sum_{k \in \mathcal{K}_m} \text{tr}(\mathbf{J}_k^{-1}) + \|\mathbf{v} - \mathbf{A}\beta\|^2, \quad (20a)$$

$$s.t. |\beta_n| = 1, \quad (20b)$$

where $\mathbf{v} = [v_{iq}]$, and $\mathbf{W} = [\mathbf{w}_{iq}], i \neq m, \forall q$. We can employ the complex circle manifold (CCM) algorithm to solve the above problem. Specifically, we first calculate the Riemannian gradient of the objective function. The Riemannian gradient of the first term is given in [10], and for the second term, it is provided in [13]. Then, the updated RIS phase shifts can be obtained based on standard procedure of CCM.

Solution to (19b): Define $\hat{g}_{iq} = (\mathbf{h}_{mq}^A)^T \text{diag}\{\beta^{t+1}\} \mathbf{a}(\theta_{im}, \phi_{im}) - \lambda_{iq}^t$ and ignore the irrelevant terms, we can translate the subproblem (19b) into

$$\min_{\mathbf{g}, \eta} \epsilon \log \eta + \frac{\gamma}{2} \sum_{i \neq m, \forall q} |g_{iq} - \hat{g}_{iq}|^2, \quad (21a)$$

$$s.t. |g_{iq}|^2 \leq \eta. \quad (21b)$$

The solution of η can be given by [13]

$$\min_{\eta} \epsilon \log \eta + \frac{\gamma}{2} \sum_{i \neq m, \forall q} \rho_{iq} (\sqrt{\eta} - |\hat{g}_{iq}|)^2, \quad (22)$$

where $\rho_{iq} = 0$ if $|\hat{g}_{iq}| < \sqrt{\eta}$, otherwise, $\rho_{iq} = 1$. Then, the solution of g_{iq} can be given as

$$g_{iq} = \begin{cases} \sqrt{\eta} \frac{\hat{g}_{iq}}{|\hat{g}_{iq}|}, & \text{if } |\hat{g}_{iq}| > \sqrt{\eta}, \\ \hat{g}_{iq}, & \text{otherwise.} \end{cases} \quad (23)$$

V. SIMULATION RESULTS

In this section, we present simulation results to demonstrate the performance of the proposed method. We consider a system of 6 RISs, and select 3 RISs to locate each user. The center transmit frequency is 28GHz, and the frequency spacing between different users is set as $\Delta f = 120\text{kHz}$. We set the cycle number as $C = 15$ and conduct $T = 500$ independent trials. For comparison, we also provided the results of an RIS-enabled NF localization method (AML in [9]) and an RIS-enabled FF localization method (ANM in [14]). Besides, the proposed algorithm is combined with pure NF or FF models to show the gain brought by the hybrid model, labeled as Proposed (NF) and Proposed (FF).

Fig. 4 (a) illustrates the average estimation RMSE versus the signal-to-noise ratio (SNR). It is evident that the proposed algorithm outperforms other compared algorithms, demonstrating its superiority. We can also see that the proposed algorithm with FF model performs worse than with the hybrid model, due to the poor estimation accuracy for NF users. Furthermore, the proposed algorithm performs worse in the NF model than in the hybrid model when the SNR is low, but slightly better when SNR is high. This is because the estimation accuracy of the range is very low at low SNR levels, especially for the FF users, which leads to poor performance during the location fusion. In contrast, the hybrid model only focuses on the more reliable angle estimation results, hence it shows higher estimation accuracy for low SNR. However, as the SNR increases, the advantage of the NF model being more accurate reveals itself. Fig. 4 (b) depicts the average estimation RMSE versus the number of cycles when SNR = 5. It can be seen that the proposed algorithm consistently outperforms other compared algorithms across all cycle numbers. The performances of the proposed algorithm with the NF and FF model are similar to Fig. 4 (a) for the same reason.

Fig. 4 (c) shows the average CPU time versus the number of RIS elements. It is observed that as the number of RIS elements increases, the CPU time for the proposed algorithms with all three models also increases. This is because the complexity of both the localization algorithm and the RIS phase shift optimization algorithm are positively related to the number of RIS elements. Additionally, we can observe that the proposed algorithm with FF model has the lowest CPU

time, while the NF model has the highest. This is attributed to the fact that the NF model treats the entire region as NF and samples the range, resulting in the most candidate locations, whereas the FF model only considers the angle, leading to the fewest candidate locations.

VI. CONCLUSION

In this paper, a multi-user hybrid NF and FF localization method based on multiple RISs has been developed. We considered a multi-user hybrid NF and FF localization scenario aided by multiple RISs, and introduced a localization protocol. A localization algorithm was designed for independent location estimation, and we proposed a location fusion algorithm to obtain the global results. The CRB of the estimated location parameters was analyzed and an ADMM-based optimization method was designed to optimize RIS phase shifts. Simulation results have shown that: 1) the proposed method outperforms the compared algorithm and can achieve sub-meter accuracy; 2) the hybrid NF and FF model has the advantages of high accuracy over pure FF model, and NF model for low SNR or number of cycles. 3) the hybrid model has lower algorithm complexity compared with NF model.

REFERENCES

- [1] R. Deng, B. Di, H. Zhang, Y. Tan, and L. Song, "Reconfigurable holographic surface-enabled multi-user wireless communications: Amplitude-controlled holographic beamforming," *IEEE Transactions on Wireless Communications*, vol. 21, no. 8, pp. 6003–6017, 2022.
- [2] R. Deng, B. Di, H. Zhang, H. V. Poor, and L. Song, "Holographic MIMO for LEO satellite communications aided by reconfigurable holographic surfaces," *IEEE Journal on Selected Areas in Communications*, vol. 40, no. 10, pp. 3071–3085, 2022.
- [3] Y. Zhang, B. Di, H. Zhang, J. Lin, Y. Li, and L. Song, "Reconfigurable intelligent surface aided cell-free mimo communications," *IEEE Wireless Communications Letters*, vol. 10, no. 4, pp. 775–779, 2021.
- [4] J. He, A. Fakhreddine, H. Wymeersch, and G. C. Alexandropoulos, "Compressed-sensing-based 3d localization with distributed passive reconfigurable intelligent surfaces," in *ICASSP 2023 - 2023 IEEE International Conference on Acoustics, Speech and Signal Processing (ICASSP)*, 2023, pp. 1–5.
- [5] Y. Zhang, Y. Liu, Y. Liu, L. Wu, Z. Zhang, and J. Dang, "Multi-ris-assisted millimeter wave single base station localization," in *2023 4th Information Communication Technologies Conference (ICTC)*, 2023, pp. 115–120.
- [6] S. Zhang, H. Zhang, B. Di, Y. Tan, M. Di Renzo, Z. Han, H. Vincent Poor, and L. Song, "Intelligent omni-surfaces: Ubiquitous wireless transmission by reflective-refractive metasurfaces," *IEEE Transactions on Wireless Communications*, vol. 21, no. 1, pp. 219–233, 2022.
- [7] M. A. ElMossallamy, H. Zhang, L. Song, K. G. Seddik, Z. Han, and G. Y. Li, "Reconfigurable intelligent surfaces for wireless communications: Principles, challenges, and opportunities," *IEEE Transactions on Cognitive Communications and Networking*, vol. 6, no. 3, pp. 990–1002, 2020.
- [8] F. Zhang, M.-M. Zhao, M. Lei, and M. Zhao, "Joint power allocation and phase-shift design for RIS-aided cooperative near-field localization," in *Proc. Int. Symp. Wirel. Commun. Syst. (ISWCS)*, Hangzhou, China, Oct. 2022.
- [9] C. Ozturk, M. F. Keskin, H. Wymeersch, and S. Gezici, "RIS-aided near-field localization under phase-dependent amplitude variations," *IEEE Trans. Wirel. Commun.*, vol. 22, no. 8, pp. 5550 – 5566, Apr. 2023.
- [10] M. Cao, H. Zhang, B. Di, and H. Zhang, "Unified near-field and far-field localization with holographic MIMO," in *2024 IEEE Wireless Communications and Networking Conference (WCNC)*, 2024, pp. 1–6.
- [11] X. Wei and L. Dai, "Channel estimation for extremely large-scale massive MIMO: Far-field, near-field, or hybrid-field?" *IEEE Commun. Lett.*, vol. 26, no. 1, pp. 177–181, 2022.
- [12] H. Xu, R. Liu, Y. Xie, J. Li, P. Zhu, and D. Wang, "Cross-region fusion and fast adaptation for multi-scenario fingerprint-based localization in cell-free massive mimo systems," *IEEE Wireless Communications Letters*, vol. 13, no. 10, pp. 2882–2886, 2024.
- [13] L. Ran, B. Sun, S. Chen, and F. Xi, "Transmit beam pattern synthesis for RIS-aided radar via sidelobe level minimization," in *2022 14th International Conference on Signal Processing Systems (ICSPPS)*. IEEE, 2022, pp. 25–30.
- [14] P. Chen, Z. Yang, Z. Chen, and Z. Guo, "Reconfigurable intelligent surface aided sparse DOA estimation method with non-ULA," *IEEE Signal Processing Letters*, vol. 28, pp. 2023–2027, 2021.